Research Square

Preprints are preliminary reports that have not undergone peer review.
They should not be considered conclusive, used to inform clinical practice,
or referenced by the media as validated information.

A Matrix-Exponential Predictive ESO-Based Control for Linear Systems with Output Delay and Uncertainty

Hakjin Choe

edu25chj0706@163.com

Kim Chaek University of Technology

Chunson Ha

Kim Chaek University of Technology

Kumchol Sin

The State of National Hydro-Meteorological Administration

• **Cholju Ri**

Kim Chaek University of Technology

Research Article

Keywords: Active Disturbance Rejection Control, Output delay, extended state observer, matrix exponential, cascade observer

Posted Date: May 21st, 2026

DOI: https://doi.org/10.21203/rs.3.rs-9600892/v1

License: This work is licensed under a Creative Commons Attribution 4.0 International License.
Read Full License

Additional Declarations: No competing interests reported.

A Matrix-Exponential Predictive ESO-Based Control for Linear Systems with Output Delay and Uncertainty

Abstract

This paper presents a matrix-exponential predictive extended state observer (MEP-ESO) based Linear Active Disturbance Rejection Control (LADRC) scheme for linear systems with output delay and uncertainty. The proposed method employs a two-stage cascade observer structure: a zeroth-order observer estimates the delayed extended state, and a first-order observer propagates the zeroth-order observer's estimate via the matrix exponential to predict the current state. This design eliminates the numerical integration required in conventional extended state predictor observer (ESPO). In addition, it uses a single gain vector shared by both cascade stages, reducing tuning to a single bandwidth parameter. Comparative simulation results verify that the proposed approach yields better tracking accuracy, shorter settling time, and stronger disturbance rejection than conventional delayed designed ADRC (DD-LADRC) and Smith predictor based ADRC (SP-LADRC). The presented method provides a simple, effective, and practical solution for robust control of delayed linear systems in industrial applications.

Keywords: Active Disturbance Rejection Control, Output delay, extended state observer, matrix exponential, cascade observer

Keywords

Active Disturbance Rejection Control (ADRC); Extended State Observer (ESO); Linear time-delay systems; Matrix exponential; Model uncertainty; Output delay

1 Introduction

Time delay and model uncertainty are key challenges commonly encountered in modern industrial control systems such as internal combustion engines [1], servo motor drives [2,3], and teleoperated systems [3]. These factors can degrade closed-loop control performance, induce oscillations, and even lead to system instability, thereby posing a significant obstacle to achieving high-precision control [4].

The extended state observer (ESO)-based active disturbance rejection control (ADRC) proposed by Han has attracted considerable attention as a powerful technique that integrates uncertainties and disturbances into a total disturbance and compensates for it [5,6]. ADRC exhibits excellent robustness and tracking performance without requiring an accurate system model, and its practicality has recently been demonstrated in various industrial systems [7–12]. However, conventional ESO cannot be directly applied to systems with output delay because the delayed measurement significantly degrades the estimation accuracy of both states and disturbances [13].

To address this problem, several delay-compensated ADRC schemes for output-delayed systems have been studied. Among them, the Smith predictor-based ADRC (SP-ADRC) and the delay-designed ADRC (DD-ADRC) are representative approaches [13]. SP-ADRC combines the delay compensation structure of the Smith predictor with ADRC [14], whereas DD-ADRC enhances

design flexibility in observer bandwidth by using a delayed control signal as the observer input [15]. Both methods provide practical frameworks for simultaneously handling output delay and uncertainties.

In addition, the extended state predictor observer (ESPO) [16,17] combines a predictor observer structure with an extended state to handle both delay and disturbances, but suffers from high computational complexity due to its integral-based prediction scheme.

Meanwhile, for the state observation problem in systems with output measurement delay, Germani et al. proposed a two-stage cascade observer. In this approach, the delayed state is first estimated, and the current state is then predicted based on that estimate. For linear systems, exponential convergence is guaranteed regardless of the delay magnitude [18]. However, this method lacks disturbance estimation capability and is therefore difficult to apply to systems with model uncertainties and external disturbances.

Recently, Bai et al. [19] proposed an extended state observer that models output delay as a transport equation and employs a PDE-backstepping technique. This method enables sophisticated delay compensation by representing the delay as a PDE state and mitigates noise amplification in measurement noise environments using a cascade structure. Nevertheless, the need for numerical PDE solutions and multi-bandwidth design demands significant computational and tuning resources.

This paper proposes a novel extended state observer (ESO) that inherits the delay compensation structure of the two-stage cascade observer while retaining the total disturbance estimation capability of conventional ESO. The proposed matrix-exponential predictive extended state observer (MEP-ESO) has the following three key features.

First, it realizes effective output delay compensation and total disturbance estimation simultaneously through a two-stage cascade structure consisting of a 0th-order observer and a 1st-order observer.

Second, instead of integral-based prediction, a matrix-exponential-based prediction mechanism is introduced to achieve delay compensation without numerical integration, which reduces computational complexity and facilitates real-time implementation.

Third, a unified gain design is applied in which both the 0th-order and 1st-order observers share a single gain vector L, thereby simplifying parameter tuning.

This study presents the structure of the proposed MEP-ESO and theoretically analyzes the dynamics and convergence of the observer error. Furthermore, comparative simulations with conventional DD-LADRC and SP-LADRC are conducted to verify that the proposed method exhibits superior robustness and control performance against output delay and model uncertainties.

The remainder of this paper is organized as follows. Section 2 defines the target system model and the extended state. Section 3 presents the structure and convergence analysis of the MEP-ESO. Section 4 describes the proposed observer-based control scheme. Section 5 provides simulation conditions and result analysis, and Section 6 concludes the paper.

2 System Model and Extended State Definition

2.1 Target System Model

A linear time-delay system including output delay (τ) and total disturbance ($f(t)$) is defined as follows:

$$\begin{cases} \dot{\boldsymbol{x}}(t) = \boldsymbol{A}\boldsymbol{x}(t) + \boldsymbol{B}u(t) + \boldsymbol{D}f(t) \\ y(t) = \boldsymbol{C}\boldsymbol{x}(t-\tau) \end{cases} \tag{1}$$

where: $\boldsymbol{x}(t) \in R^n$ is the system state vector, $u(t) \in R$ is the control input, $y(t) \in R$ is the delayed output signal (τ is the output delay time, assumed constant), $f(t) \in R$ is the total disturbance including model uncertainties and external disturbances, and $\boldsymbol{A} \in R^{n\times n}$, $\boldsymbol{B} = \begin{bmatrix} b_{n-1} \\ \vdots \\ b_0 \end{bmatrix} \in R^{n\times 1}$, $\boldsymbol{C} \in R^{1\times n}$, $\boldsymbol{D} \in R^{n\times 1}$ are known constant system parameter matrices.

Assumption 1:

The pair $(A,\ C)$ is completely observable, ensuring the feasibility of state estimation for the proposed observer design.

Assumption 2.

The total disturbance $f(t)$ is continuously differentiable and its time derivative $\dot{f}(t)$ is bounded.

2.2 Extended State Definition

Utilizing the core principle of ESO, the system state and total disturbance are integrated into an extended state:

$$\boldsymbol{x}_e(t) = \begin{bmatrix} \boldsymbol{x}(t) \\ f(t) \end{bmatrix} \in R^{n+1}$$

In this case, the state equation of the extended system is re-expressed as:

$$\begin{cases} \dot{\boldsymbol{x}}_e(t) = \boldsymbol{A}_e\boldsymbol{x}_e(t) + \boldsymbol{B}_e u(t) \\ y(t) = \boldsymbol{C}_e\boldsymbol{x}_e(t-\tau) \end{cases} \tag{2}$$

where $\boldsymbol{A}_e = \begin{bmatrix} \boldsymbol{A} & \boldsymbol{D} \\ \boldsymbol{0}_{1\times n} & 0 \end{bmatrix} \in R^{(n+1)\times(n+1)}$ is the extended state matrix, $\boldsymbol{B}_e = \begin{bmatrix} \boldsymbol{B} \\ 0 \end{bmatrix} \in R^{(n+1)\times 1}$ is the extended input matrix, and $\boldsymbol{C}_e = [\boldsymbol{C}\ 0] \in R^{1\times(n+1)}$ is the extended output matrix. By estimating the extended state $\boldsymbol{x}_e(t)$, both the system state $\boldsymbol{x}(t)$ and total disturbance $f(t)$ can be obtained.

3 Matrix Exponential Predictive Extended State Observer

The proposed MEP-ESO estimates the current state $\boldsymbol{x}_e(t)$ from the delayed output $y(t) = \boldsymbol{C}_e\boldsymbol{x}_e(t-\tau)$based on the two-stage cascade structure of the chain observer. The structure and derivation process of the 0th-order observer and 1st-order observer are detailed as follows.

3.1 0th-Order Observer (Delayed State Estimation)

The 0th-order observer for estimating the extended state $\boldsymbol{x}_e(t\text{-}\tau)$ at time $t\text{-}\tau$ is defined as:

$$\dot{\boldsymbol{z}}_0(t) = \boldsymbol{A}_e\boldsymbol{z}_0(t) + \boldsymbol{B}_e u(t-\tau) + \boldsymbol{L}(y(t) - \boldsymbol{C}_e\boldsymbol{z}_0(t)) \tag{3}$$

where $\boldsymbol{z}_0(t)$ is the estimated value of the extended state $\boldsymbol{x}_e(t-\tau)$ at time $t-\tau$, and $\boldsymbol{L} \in R^{(n+1)\times 1}$ is the observer gain vector.

3.2 1st-Order Observer (Current State Estimation)

The 1st-order observer for estimating the current state $\boldsymbol{x}_e(t)$ at time t is derived using the estimated value from the 0th-order observer and matrix exponential-based state transition. First, a basic equation utilizing the state transition relationship of linear systems is derived, followed by defining the observer structure and deriving the final dynamic equation.

3.2.1 Derivation Process of the 1st-Order Observer

For a linear system, the extended state $\boldsymbol{x}_e(t)$ at the current time t and the extended state $\boldsymbol{x}_e(t-\tau)$ at the past time $t-\tau$ satisfy the following relationship. This equation models the dynamic changes of the system during the delay time τ using the matrix exponential $e^{\boldsymbol{A}_e\tau}$, serving as the basis for predicting the current state from the past state:

$$\boldsymbol{x}_e(t) = e^{\boldsymbol{A}_e\tau}\boldsymbol{x}_e(t-\tau) + \int_{t-\tau}^{t} e^{\boldsymbol{A}_e(t-s)}\boldsymbol{B}_e u(s)ds \tag{4}$$

Since the estimated value $\boldsymbol{z}_0(t)$ of the 0th-order observer converges to $\boldsymbol{x}_e(t-\tau)$, $\boldsymbol{z}_0(t)$ can be used as a substitute for $\boldsymbol{x}_e(t-\tau)$. Based on this, the estimated value $\boldsymbol{z}_1(t)$ of the 1st-order observer is defined with the same structure as Equation (4), enabling prediction of the current state from the past estimated value:

$$\boldsymbol{z}_1(t) = e^{\boldsymbol{A}_e\tau}\boldsymbol{z}_0(t) + \int_{t-\tau}^{t} e^{\boldsymbol{A}_e(t-s)}\boldsymbol{B}_e u(s)ds \tag{5}$$

Differentiating both sides of Equation (5) yields:

$$\dot{\boldsymbol{z}}_1(t) = e^{\boldsymbol{A}_e\tau}\dot{\boldsymbol{z}}_0(t) + \boldsymbol{B}_e u(t) - e^{\boldsymbol{A}_e\tau}\boldsymbol{B}_e u(t-\tau) + \boldsymbol{A}_e\int_{t-\tau}^{t} e^{\boldsymbol{A}_e(t-s)}\boldsymbol{B}_e u(s)ds \tag{6}$$

The integral term in Equation (6) is substituted by deriving the integral term from Equation (5), resulting in:

$$\dot{\boldsymbol{z}}_1(t) = \boldsymbol{A}_e\boldsymbol{z}_1(t) + \boldsymbol{B}_e u(t) + e^{\boldsymbol{A}_e\tau}(\dot{\boldsymbol{z}}_0(t) - \boldsymbol{A}_e\boldsymbol{z}_0(t) - \boldsymbol{B}_e u(t-\tau)) \tag{7}$$

Finally, the dynamic equation of the 1st-order observer is obtained by substituting and rearranging the dynamics of the 0th-order observer (Equation (3)). Through this process, the estimation error of the 0th-order observer is reflected as a compensation term in the 1st-order observer, achieving a structure that improves the accuracy of current state estimation:

$$\dot{\boldsymbol{z}}_1(t) = \boldsymbol{A}_e\boldsymbol{z}_1(t) + \boldsymbol{B}_e u(t) + e^{\boldsymbol{A}_e\tau}\boldsymbol{L}(y(t) - \boldsymbol{C}_e\boldsymbol{z}_0(t)) \tag{8}$$

3.2.2 Significance of the 1st-Order Observer

1. $\boldsymbol{z}_1(t)$ is the value obtained by "predicting the current time" from the estimated value $\boldsymbol{z}_0(t)$ of the 0th-order observer using matrix exponential.
2. The compensation term $e^{\boldsymbol{A}_e\tau}\boldsymbol{L}\big(y(t) - \boldsymbol{C}_e\boldsymbol{z}_0(t)\big)$ transmits the estimation error of the 0th-order observer to the current time, improving the estimation accuracy of $\boldsymbol{z}_1(t)$.

3.3 Key Features of the Proposed MEP-ESO

The derived MEP-ESO addresses output delay and model uncertainties simultaneously through a cascade structure of 0th-order and 1st-order observers. It estimates the extended state including total disturbance with a single observer, replacing the integral-based predictive terms of ESPO with a simplified predictive mechanism using matrix exponential to reduce computational complexity. Additionally, the two-stage estimation structure accurately

reconstructs the current state from the delayed output, and the extended state structure ensures robustness against model uncertainties.

3.4 Convergence Analysis of MEP-ESO

3.4.1 Definition of Estimation Errors

Based on the observer structure in Section 3, the estimation errors are defined as follows:

$$\boldsymbol{e}_0(t) = \boldsymbol{x}_e(t-\tau) - \boldsymbol{z}_0(t) \tag{9}$$

$$\boldsymbol{e}_1(t) = \boldsymbol{x}_e(t) - \boldsymbol{z}_1(t) \tag{10}$$

where $\boldsymbol{e}_0(t)$ is the delayed state estimation error of the 0th-order observer, and $\boldsymbol{e}_1(t)$ is the current state estimation error of the 1st-order observer.

3.4.2 Error Dynamics of the 0th-Order Observer

Using Equation (3) and the extended system model $\dot{\boldsymbol{x}}_e(t-\tau) = \boldsymbol{A}_e\boldsymbol{x}_e(t-\tau) + \boldsymbol{B}_e u(t-\tau)$, the dynamics of $\boldsymbol{e}_0(t)$ are derived as:

$$\dot{\boldsymbol{e}}_0(t) = \dot{\boldsymbol{x}}_e(t-\tau) - \dot{\boldsymbol{z}}_0(t) = (\boldsymbol{A}_e - \boldsymbol{L}\boldsymbol{C}_e)\boldsymbol{e}_0(t) \tag{11}$$

Since $\boldsymbol{A}_e - \boldsymbol{L}\boldsymbol{C}_e$ is a Hurwitz matrix, $\boldsymbol{e}_0(t)$ converges exponentially to 0, satisfying the following inequality:

$$|\boldsymbol{e}_0(t)| \leq \beta_0 \boldsymbol{e}^{-\lambda_0 t}, \forall t \geq 0 \tag{12}$$

where $\beta_0 = |\boldsymbol{e}_0(0)|$ and $\lambda_0 > 0$ is a positive constant determining the convergence rate.

3.4.3 Error Dynamics of the 1st-Order Observer

Rearranging $\boldsymbol{e}_1(t)$ using Equation (5) derived in Section 3 and the system state transition Equation (4):

$$\boldsymbol{e}_1(t) = e^{\boldsymbol{A}_e\tau}\boldsymbol{e}_0(t) \tag{13}$$

Since $\boldsymbol{e}_0(t)$ converges to zero exponentially and $e^{\boldsymbol{A}_e\tau}$ is a constant matrix, $\boldsymbol{e}_1(t)$ also converges to zero exponentially.

This guarantees the exponential convergence of the proposed MEP-ESO.

4 MEP-ESO based Control System

4.1 Control Law

Based on the MEP-ESO designed in Section 3, a linear active disturbance rejection control

law is constructed as follows:

$$\begin{cases} \dot{\boldsymbol{z}}_0(t) = \boldsymbol{A}_e \boldsymbol{z}_0(t) + \boldsymbol{B}_e u(t-\tau) + \boldsymbol{L}(y(t) - \boldsymbol{C}_e \boldsymbol{z}_0(t)) \\ \dot{\boldsymbol{z}}_1(t) = \boldsymbol{A}_e \boldsymbol{z}_1(t) + \boldsymbol{B}_e u(t) + e^{\boldsymbol{A}_e \tau} \boldsymbol{L}(y(t) - \boldsymbol{C}_e \boldsymbol{z}_0(t)) \\ u(t) = k_s r(t) - \boldsymbol{K}_0 \boldsymbol{z}_1(t) \end{cases} \tag{14}$$

Where $r(t)$ is the reference command, k_s is the static gain compensation, and) $\boldsymbol{K}_0 \in R^{1\times(n+1)}$ is the state feedback gain vector.

The overall block diagram of the closed-loop control system based on (14) is illustrated in Fig. 1

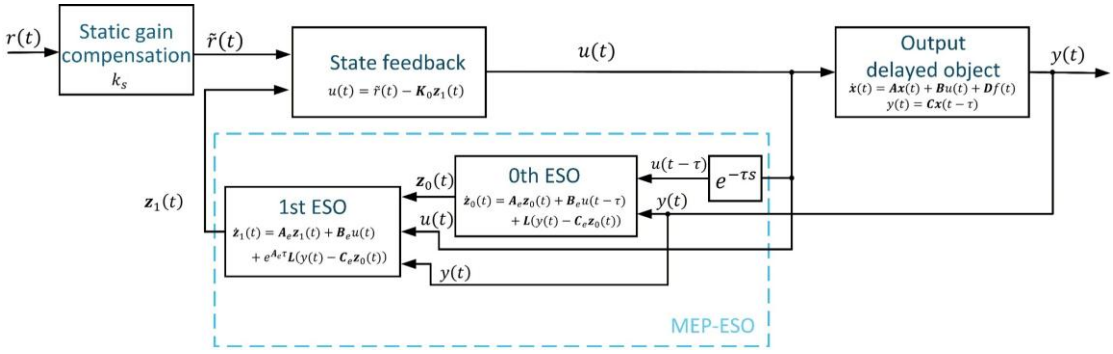


Fig. 1: Overall control system structure based on MEP-ESO

4.2 Observer and Controller Gain Design

4.2.1 Observer Gain Vector Design

The gain vector $\boldsymbol{L}$ is designed such that $\boldsymbol{A}_e - \boldsymbol{L}\boldsymbol{C}_e$ is a Hurwitz matrix, guaranteeing the exponential convergence of the estimation error of the 0th-order observer. In this study, the bandwidth parameterization method [20] is applied, placing all poles of the observer at the observer bandwidth ω_0.

When all poles of the observer are placed at the observer bandwidth ω_0, the characteristic equation of the observer should be $\psi(s) = (s + \omega_0)^{n+1}$. At this time, $\boldsymbol{L}$ is calculated using Ackermann's formula:

$$\boldsymbol{L} = \psi(\boldsymbol{A}_e) \begin{bmatrix} \boldsymbol{C}_e \\ \boldsymbol{C}_e \boldsymbol{A}_e \\ \vdots \\ \boldsymbol{C}_e \boldsymbol{A}_e^n \end{bmatrix}^{-1} \begin{bmatrix} 0 \\ 0 \\ \vdots \\ 1 \end{bmatrix} \tag{15}$$

4.2.2 Controller Gain Design

The controller gain K_0 is determined based on the bandwidth parameterization method, with the derivation process from the controller bandwidth ω_c to the gain referencing the pole placement framework in [21].

Meanwhile, a key practical relationship exists between the controller bandwidth ω_c and the observer bandwidth ω_0: the observer bandwidth must be larger than the controller bandwidth.

As a standard guideline in linear active disturbance rejection control [20], ω_0 is generally set to 3~5 times ω_c to ensure fast enough state and disturbance estimation.

4.2.3 Static Gain Compensation

To ensure $\boldsymbol{r} = \boldsymbol{y}$ in steady state, the gain k_s must be set to the inverse of the loop gain using [22]

$$k_s = \frac{1}{-\boldsymbol{C}(\boldsymbol{A} - \boldsymbol{B}\bar{\boldsymbol{K}}_{\boldsymbol{0}})^{-1}\boldsymbol{B}} \tag{16}$$

where $\bar{\boldsymbol{K}}_{\boldsymbol{0}}$ is related to the state feedback gain vector $\boldsymbol{K}_{\boldsymbol{0}}$ by

$$\boldsymbol{K}_{\boldsymbol{0}} = [k_1 \quad k_2 \quad \cdots \quad k_n \quad 1]/b_0 = [\bar{\boldsymbol{K}}_{\boldsymbol{0}} \quad 1/b_0] \tag{17}$$

5 Simulation Validation

5.1 Basic System Model (Second-Order Inertial Delay System)

A second-order inertial delay system is used for simulation validation, with the state equation defined as follows (reference model):

$$\begin{cases} \dot{x}_1(t) = x_2(t) \\ \dot{x}_2(t) = -\dfrac{k}{m}x_1(t) - \dfrac{c}{m}x_2(t) + \dfrac{1}{m}u(t) + f(t) \\ y(t) = x_1(t-\tau) \end{cases} \tag{18}$$

Reference parameters:

- Mass m=1 kg, damping coefficient c=2 N·s/m, stiffness coefficient k=5 N/m
- Output delay τ=0.1 s
- Total disturbance $f(t)$: 1 N step disturbance applied at t=8 s

5.2 Parameter Setting of Comparative Observers and Simulation System Configuration

For simulation validation, the proposed MEP-ESO-based LADRC is compared with two conventional methods:

- Delayed Designed Linear ADRC (DD-LADRC)
- Smith Predictor-based Linear ADRC (SP-LADRC)

5.2.1 Parameter settings

Extended state matrix:

$$\boldsymbol{A}_e=\begin{bmatrix}0 & 1 & 0\\ -5 & -2 & 1\\ 0 & 0 & 0\end{bmatrix}$$

Extended input matrix $\boldsymbol{B}_e = [0\ 1\ 0]^T$, extended output matrix $\boldsymbol{C}_e = [1\ 0\ 0]$

Matrix exponential $e^{\boldsymbol{A}_e\tau}$ (τ=0.1 s):

$$e^{\boldsymbol{A}_e\tau} = \begin{bmatrix}0.9767 & 0.0899 & 0.0047\\ -0.4494 & 0.7969 & 0.0899\\ 0 & 0 & 1.0000\end{bmatrix}$$

Observer and controller gains are designed based on the bandwidth parameterization method. To ensure fairness of comparison, the observer gain vector and controller gain vector are set identically for all methods. The controller bandwidth is determined as ω_c=0.6 based on the required transient response, and the observer bandwidth is set as ω_0=3 according to ω_0=(3~5)ω_c. The controller gain and observer gain vector are as follows:

$$\boldsymbol{K}_0 = [4.64 \quad 0.8 \quad 1], \quad \boldsymbol{L} = \begin{bmatrix}7\\ 8\\ 27\end{bmatrix}$$

5.2.2 Simulation environment

Simulations are performed in MATLAB/SIMULINK with a simulation time of 20 s and a fixed step size of 0.01 s.

5.3 Simulation Conditions

Simulations are conducted under five cases to verify the impact of model uncertainties (Table 1).

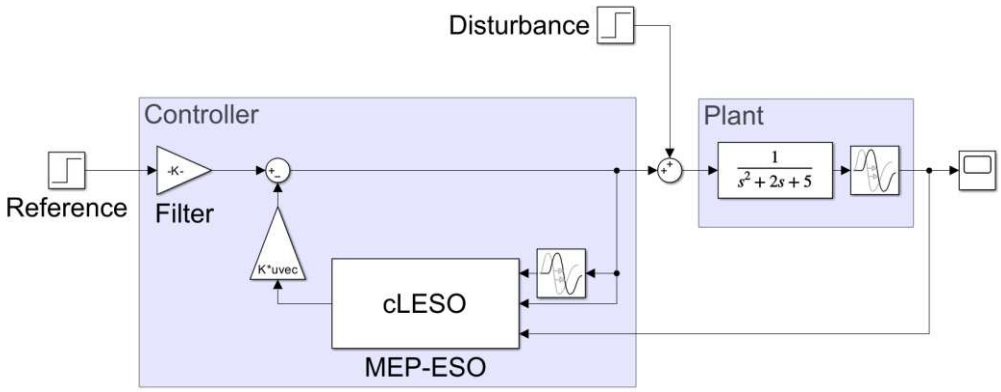


Fig. 2: SIMULINK simulation configuration of the proposed method.

Table 1 Simulation conditions for each case

Case	Simulation Conditions
1	Nominal model, 1 N disturbance applied at t = 8 s

2	Nominal model with 30% increase in m (m = 1.3 kg), 1 N disturbance applied at t = 8 s
3	Nominal model with 30% decrease in c (c = 1.4 N·s/m), 1 N disturbance applied at t = 8 s
4	Nominal model with 30% decrease in k (k = 3.5 N/m), 1 N disturbance applied at t = 8 s
5	Nominal model with 20% increase in m, 20% decrease in c, and 20% decrease in k (m = 1.2 kg, c = 1.6 N·s/m, k = 4 N/m), 1 N disturbance applied at t = 10 s

5.4 Simulation Results and Analysis

5.4.1 Case 1: Nominal Model

In the nominal model, the proposed method exhibits similar IAE and settling time to SP-LADRC, with the smallest overshoot, demonstrating stable response (Fig. 3 and Table 2). Although the disturbance rejection time is slightly longer than that of DD-LADRC, overall control performance is excellent.

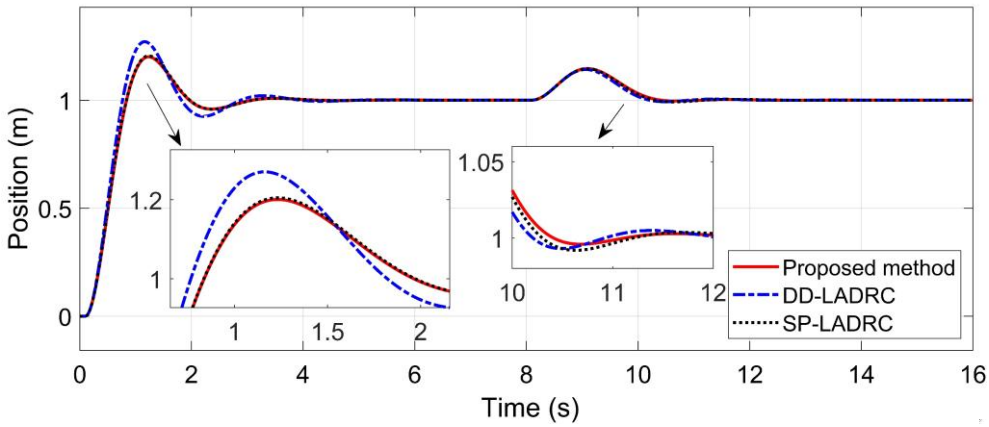


Fig. 3: Response curve for the nominal model. The solid line represents the proposed MEP-ESO, dashed line represents DD-LADRC, and dotted line represents SP-LADRC.

Table 2 Response characteristics for the nominal model

Performance Index	DD-LADRC	SP-LADRC	Proposed Method (MEP-ESO)

IAE	0.884	0.855	0.853
Overshoot (%)	27.1	20.5	20.0
Settling Time (s)	3.35	2.78	2.77
Disturbance Rejection Time (s)	1.97	2.06	2.10

5.4.2 Case 2: 30% Increase in *m*

Under conditions of increased inertia due to mass increase, the proposed method exhibits the smallest IAE and shortest settling time, demonstrating robustness against model uncertainties (Fig. 4 and Table 3). In particular, the disturbance rejection time is significantly improved to 2.87 s compared to conventional methods, verifying fast response capability to disturbances.

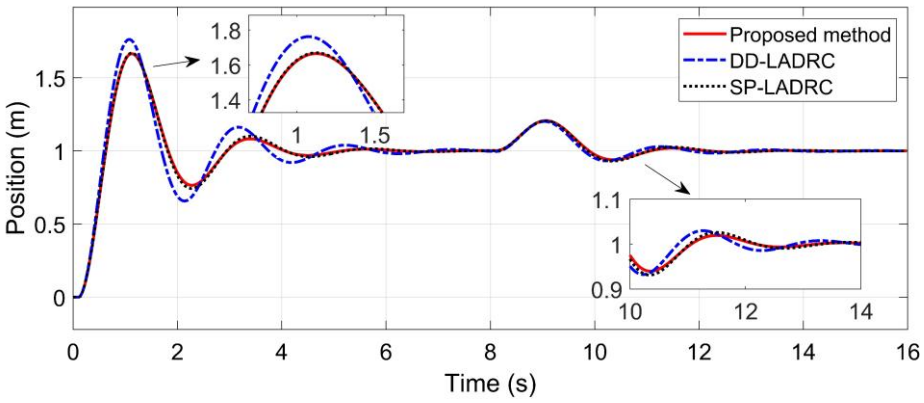


Fig. 4: Response curve with 30% increase in *m*. The solid line represents the proposed MEP-ESO, dashed line represents DD-LADRC, and dotted line represents SP-LADRC.

Table 3 Response characteristics with 30% increase in *m*

Performance Index	DD-LADRC	SP-LADRC	Proposed Method (MEP-ESO)
IAE	1.616	1.485	1.432
Overshoot (%)	76.2	66.9	66.5
Settling Time (s)	5.58	4.94	4.81

Disturbance Rejection Time (s)	3.55	3.75	2.87

5.4.3 Case 3: 30% Decrease in *c*

Under conditions of increased vibration due to decreased damping coefficient, the proposed method exhibits the smallest overshoot and a settling time shortened by approximately 15% compared to conventional methods (4.80 s) (Fig. 5 and Table 4). The minimum IAE also confirms its excellent steady-state and transient control performance.

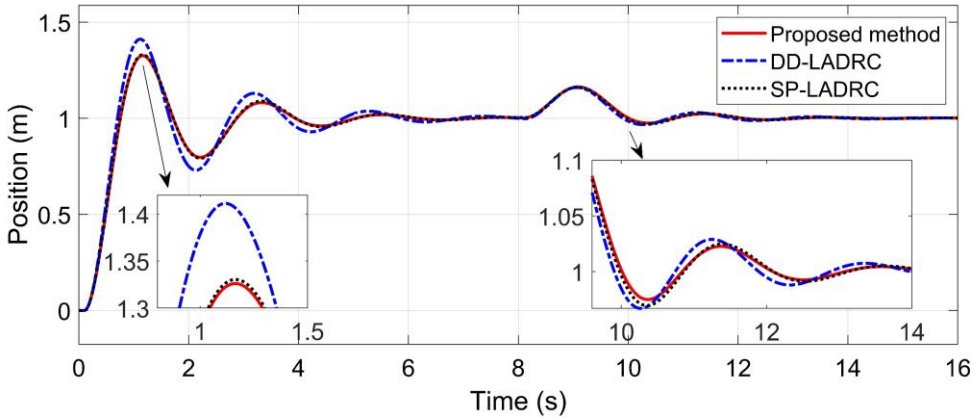


Fig. 5: Response curve with 30% decrease in *c*. The solid line represents the proposed MEP-ESO, dashed line represents DD-LADRC, and dotted line represents SP-LADRC.

Table 4 Response characteristics with 30% decrease in *c*

Performance Index	DD-LADRC	SP-LADRC	Proposed Method (MEP-ESO)
IAE	1.275	1.159	1.137
Overshoot (%)	41.1	33.0	32.6
Settling Time (s)	5.63	5.62	4.80
Disturbance Rejection Time (s)	3.55	3.64	3.56

5.4.4 Case 4: 30% Decrease in *k*

Under conditions of decreased stiffness coefficient, SP-LADRC exhibits a significantly increased settling time of 5.14 s, while the proposed method maintains a stable response with

4.01 s (Fig. 6 and Table 5). The smallest overshoot also demonstrates robustness against changes in system stiffness.

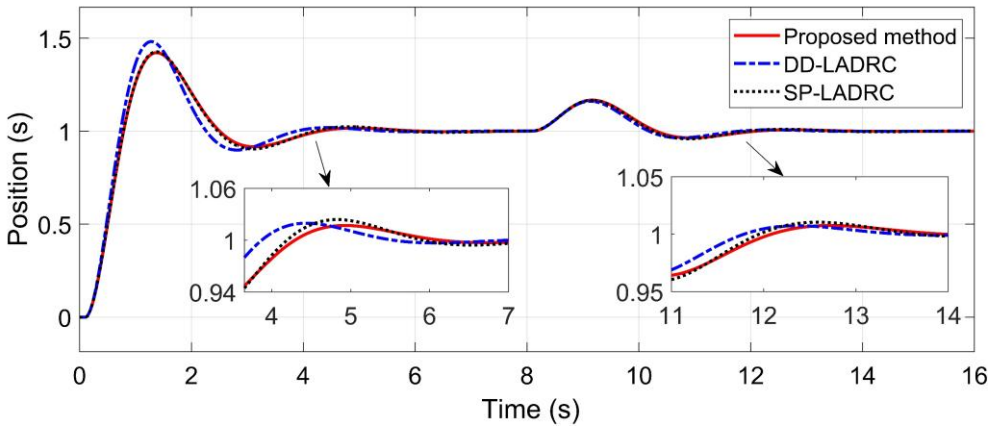


Fig. 6: Response curve with 30% decrease in k. The solid line represents the proposed MEP-ESO, dashed line represents DD-LADRC, and dotted line represents SP-LADRC.

Table 5 Response characteristics with 30% decrease in k

Performance Index	DD-LADRC	SP-LADRC	Proposed Method (MEP-ESO)
IAE	1.257	1.309	1.285
Overshoot (%)	48.2	42.7	42.2
Settling Time (s)	3.65	5.14	4.01
Disturbance Rejection Time (s)	3.27	3.50	3.52

5.4.5 Case 5: Combined Variations of *m*, *c*, and *k*

As shown in Fig. 7 and Table 6, the proposed method achieves the smallest IAE (1.882) and shortest settling time (6.55 s) under combined parameter uncertainties. Its disturbance rejection time (4.14 s) is also faster than DD-LADRC and SP-LADRC, confirming robust performance against complex model variations.

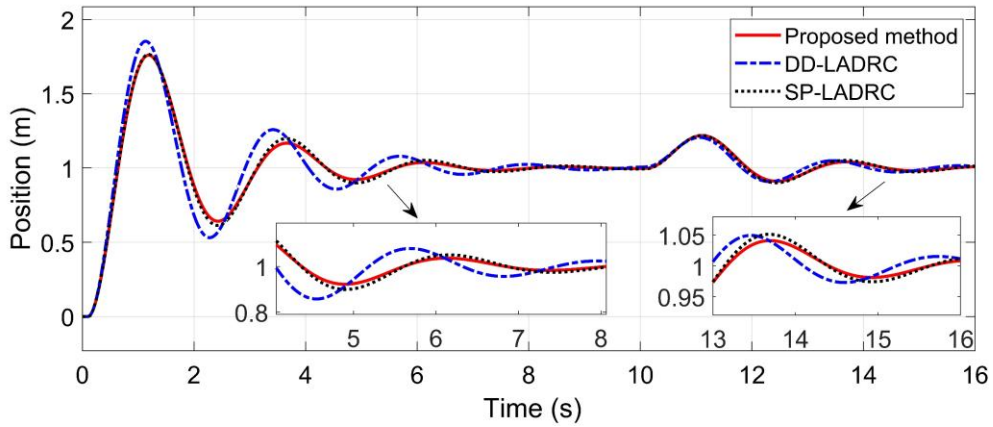


Fig. 7: Response curve with combined variations of m, c, and k. The solid line represents the proposed MEP-ESO, dashed line represents DD-LADRC, and dotted line represents SP-LADRC.

Table 6 Response characteristics under combined model uncertainties

Performance Index	DD-LADRC	SP-LADRC	Proposed Method (MEP-ESO)
IAE	2.110	1.993	1.882
Overshoot (%)	85.3	76.5	76.0
Settling Time (s)	8.19	7.67	6.55
Disturbance Rejection Time (s)	4.87	5.21	4.14

5.5 Summary of Simulation Results

The proposed MEP-ESO-based LADRC exhibits the following advantages:

- In the nominal model, it achieves performance similar to conventional SP-LADRC with minimized overshoot.
- Under conditions of single parameter uncertainties (mass, damping, stiffness) and combined uncertainties, it consistently achieves the minimum IAE and shortest settling time.
- It exhibits excellent disturbance rejection capability, particularly outperforming conventional methods under increased inertia or combined uncertainties.

6 Conclusion

This paper has proposed a Matrix Exponential Predictive Extended State Observer (MEP-ESO)-based LADRC for simultaneous handling of output delay and model uncertainties.

The MEP-ESO employs a two-stage cascade structure: a zeroth-order observer estimates the delayed extended state, and a first-order observer propagates this estimate via the matrix exponential to predict the current state. This design eliminates numerical integration and uses a single gain vector for both stages, reducing observer tuning to one bandwidth parameter.

In addition, convergence analysis proved exponential convergence, showing that the current-state estimation error inherits exponential convergence directly from the delayed-state error via the matrix exponential.

Simulations on a second-order system under five uncertainty scenarios (nominal, ±30% parameter variations, combined) demonstrated that the MEP-ESO based control scheme achieves smaller IAE, up to 20% shorter settling time, and faster disturbance rejection than conventional DD-LADRC and SP-LADRC.

Future work will extend the method to time-varying delays and nonlinear systems, and validate its performance on hardware platforms.

References

1. Song K, Hao T, Xie H (2018) Disturbance rejection control of air–fuel ratio with transport-delay in engines. Control Eng Pract 79:36-49. https://doi.org/10.1016/j.conengprac.2018.06.009
2. Ma M, Yao S, Ma W (2025) Study on control approaches for servo systems exhibiting uncertain time delays. Mach 13:264. https://doi.org/10.3390/machines13040264
3. Na J, Ren X, Costa-Castelló R, Guo Y (2014) Repetitive control of servo systems with time delays. Robot Auton Syst 62:319–329. http://dx.doi.org/10.1016/j.robot.2013.09.010
4. Niculescu SI (2001) Delay Effects on Stability: A Robust Control Approach. Springer, London. https://doi.org/10.1007/1-84628-553-4
5. Han JQ (1998) Auto disturbance rejection controller and its applications. Control Decis 13:19–23 [in Chinese]
6. Han J (2009) From PID to active disturbance rejection control. IEEE Trans Ind Electronics 56(3):900–906. https://doi.org/10.1109/TIE.2008.2011621
7. Su Z, Sun L, Xue W, Lee KY (2023) A review on active disturbance rejection control of power generation systems: fundamentals, tunings and practices. Control Eng Pract 141:105716. https://doi.org/10.1016/j.conengprac.2023.105716
8. Yao J, Deng W (2017) Active disturbance rejection adaptive control of hydraulic servo systems. IEEE Trans Ind Electronics 64(10):8023–8032. https://doi.org/10.1109/TIE.2017.2694382

9. Wang H, Meng Y, Sun J, Zhang L, Zhang H, Zheng S (2026) Dual-coil active disturbance rejection control for compact MEG measurement systems. Control Eng Pract 170:106833. https://doi.org/10.1016/j.conengprac.2026.106833
10. Choe H, Jang K, Ham K, Kang C (2025) A cascade control scheme with T-S fuzzy model-assisted linear active disturbance rejection controller for position tracking of cart inverted pendulum. Int J Dyn Control 13:97. https://doi.org/10.1007/s40435-025-01617-6
11. Kang JS, Paek SY, Rim CR (2022) A design of active disturbance rejection control with higher convergence rate and its application in inertia wheel pendulum stabilization. J Braz Soc Mech Sci Eng 44:477. https://doi.org/10.1007/s40430-022-03771-w
12. Tang W, Ma J, Wei Z, Gao H (2026) Active disturbance rejection control of hypersonic vehicles based on modified deep deterministic policy gradient. Int J Dyn Control 14:64. https://doi.org/10.1007/s40435-026-02008-1
13. Fu C, Tan W (2020) Linear active disturbance rejection control for processes with time delays: IMC interpretation. IEEE Access 8:16606–16617. https://doi.org/10.1109/ACCESS.2020.2967806
14. Zheng Q, Gao Z (2014) Predictive active disturbance rejection control for processes with time delay. ISA Trans 53:873–881. http://dx.doi.org/10.1016/j.isatra.2013.09.021
15. Zhao S, Gao Z (2014) Modified active disturbance rejection control for time-delay systems. ISA Trans 53:882–888. http://dx.doi.org/10.1016/j.isatra.2013.09.013
16. Wu Y, Gao P, Wu R, Du J (2023) ESPO based course-tracking control of ships with input delay. Int J Control Autom Syst 21(3):755–763. http://dx.doi.org/10.1007/s12555-021-0782-9
17. Nahri SNF, Du S, van Wyk BJ (2023) Predictive extended state observer-based active disturbance rejection control for systems with time delay. Machines 11:144. https://doi.org/10.3390/machines11020144
18. Germani A, Manes C, Pepe P (2000) State observation of nonlinear systems with delayed output measurements. IFAC Proc Vol 33(23):115-120. https://doi.org/10.1016/S1474-6670(17)36926-4
19. Bai Y, Yao J, Hu J (2023) A new state observer for active disturbance rejection control with measurement noise and output delay using the PDE-backstepping predictor. ISA Trans 142:562–572. https://doi.org/10.1016/j.isatra.2023.07.013
20. Gao Z (2003) Scaling and bandwidth-parameterization based controller tuning. In: Proceedings of 2003 American control conference. https://doi.org/10.1109/ACC.2003.1242516
21. Fu C, Tan W (2016) Tuning of linear ADRC with known plant information. ISA Trans 65:384–393. http://dx.doi.org/10.1016/j.isatra.2016.06.016
22. Herbst G, Madonski R (2025) Active disturbance rejection control: from principles to practice. Birkhäuser, Cham. https://doi.org/10.1007/978-3-031-72687-3